Analytical and Numerical Normal Solutions of the Boltzmann Equation for Highly Nonequilibrium Fourier and Couette Flows

M. A. Gallis[*], J. R. Torczynski[*], D. J. Rader[*], M. Tij[†], and A. Santos[¶]

[*]*Engineering Sciences Center, Sandia National Laboratories, Albuquerque, New Mexico 87185 USA*
[†]*Département de Physique, Université Moulay Ismaïl, Meknès, Morocco*
[¶]*Departamento de Física, Universidad de Extremadura, E-06071 Badajoz, Spain*

Abstract. Normal solutions of the Boltzmann equation for a single-species monatomic gas in Fourier flow (uniform heat flux) or Couette flow (uniform shear stress) are found in terms of the heat-flux and shear-stress Knudsen numbers. Analytical solutions for Maxwell molecules at finite Knudsen numbers are found using a moment-hierarchy (MH) method, and corresponding numerical solutions are obtained using the Direct Simulation Monte Carlo (DSMC) method of Bird. The MH and DSMC results both indicate that the effective thermal conductivity and the effective viscosity for Maxwell molecules are independent of the heat-flux Knudsen number but decrease as the shear-stress Knudsen number is increased. Additional DSMC simulations indicate that these transport properties for hard-sphere molecules decrease as either the heat-flux Knudsen number or the shear-stress Knudsen number is increased.

INTRODUCTION

In a "normal" solution of the Boltzmann equation (BE) [1], temporal and spatial variations occur entirely through a functional dependence on the hydrodynamic fields (number density, temperature, and velocity). In continuum situations, departure from equilibrium is small, so the velocity distribution function can be represented as an expansion about the equilibrium distribution in terms of the local heat-flux and shear-stress Knudsen numbers. Chapman-Enskog (CE) theory [1] provides such a representation but is limited to small local Knudsen numbers.

In the case of Maxwell molecules [1], moments of the collision term can be determined directly from moments of the velocity distribution function without detailed knowledge of this function. This property allows a hierarchy of moment equations to be derived from the BE, and this system of equations can be solved recursively to obtain normal solutions at arbitrary Knudsen numbers. Several exact solutions for uniform heat flux and uniform shear stress based on this moment-hierarchy (MH) method have been derived, and efficient algorithms for computing these moments symbolically and numerically have been reported [2-6].

The Direct Simulation Monte Carlo (DSMC) method of Bird [7] is a numerical method for simulating nonequilibrium gas behavior. In brief, computational molecules statistically mimic the behavior of real molecules. Wagner [8] provides a rigorous proof that DSMC produces a solution to the Boltzmann equation in the limit of vanishing discretization and stochastic errors. DSMC can simulate Maxwell and other molecules at small and finite local Knudsen numbers and therefore can determine normal solutions numerically [9-13].

Herein, Fourier flow and Couette flow at nonequilibrium conditions are investigated. In Fourier flow, the gas experiences a uniform heat flux, whereas in Couette flow, the gas experiences a uniform shear stress. These flows are produced in DSMC simulations by confining the gas between two parallel, solid walls at fixed, uniform conditions. To ensure that a normal solution is obtained in the central region of the domain, the walls are separated by ~40 mean free paths. For Maxwell molecules, MH analytical solutions and DSMC numerical solutions are compared. For hard-sphere molecules, only DSMC numerical solutions are presented since no analytical results are available. The thermal conductivity, the viscosity, and the Sonine-polynomial coefficients of the velocity distribution function are determined as functions of the heat-flux and shear-stress Knudsen numbers.

MOMENT-HIERARCHY METHOD

Chapman-Enskog (CE) theory provides the normal solution of the BE as an expansion in the heat-flux (q) and shear-stress (τ) Knudsen numbers [1] $\mathrm{Kn}_q = q/(mnc_m^3)$ and $\mathrm{Kn}_\tau = \tau/(mnc_m^2)$, where $c_m = (2k_BT/m)^{1/2}$. Table 1 contains Maxwell and hard-sphere CE values for the infinite-to-first-approximation ratios of viscosity, thermal conductivity, and self-diffusion coefficient (μ_∞/μ_1 , K_∞/K_1 , and D_∞/D_1 , respectively) and for the heat-flux and shear-stress Sonine-polynomial-coefficient ratios (a_k/a_1 and b_k/b_1) in the limit of small Knudsen numbers [11-13].

The Moment-Hierarchy (MH) method is able to extend CE theory to finite Knudsen numbers for Maxwell molecules because their collision rate is independent of relative speed. This property allows the BE to be represented as an infinite hierarchy of moment equations [4-5]. Moments of the BE relate moments of the distribution function f to moments of the collision operator $J[\mathbf{c} \mid f, f]$, where their nondimensional forms are given below:

$$M_{k_1k_2k_3} = \int \tilde{c}_x^{k_1}\tilde{c}_y^{k_2}\tilde{c}_z^{k_3}\tilde{f}[\tilde{\mathbf{c}}]d\tilde{\mathbf{c}} = \left\langle \tilde{c}_x^{k_1}\tilde{c}_y^{k_2}\tilde{c}_z^{k_3} \right\rangle, \quad J_{k_1k_2k_3} = \int \tilde{c}_x^{k_1}\tilde{c}_y^{k_2}\tilde{c}_z^{k_3} J[\tilde{\mathbf{c}} \mid \tilde{f}, \tilde{f}]d\tilde{\mathbf{c}}, \quad \tilde{\mathbf{c}} = \mathbf{c}/c_m , \quad \tilde{f} = fc_m^3/n . \tag{1}$$

For Maxwell molecules, the $J_{k_1k_2k_3}$ can be expressed as bilinear combinations of the $M_{k_1k_2k_3}$ [4-5]. This property enables a normal solution to be obtained recursively [2-5]. In this solution, the pressure $p = nk_BT$ is uniform, the moments $M_{k_1k_2k_3}$ are polynomials in Kn_q of degree $k_1 + k_2 + k_3 - 2 \geq 0$, and the coefficients $\mu^{(j)}_{k_1k_2k_3}$ can be represented by infinite expansions in powers of Kn_τ :

$$M_{k_1k_2k_3}[\mathrm{Kn}_q, \mathrm{Kn}_\tau] = \sum_{j=0}^{k_1+k_2+k_3-2} \mu^{(j)}_{k_1k_2k_3}[\mathrm{Kn}_\tau]\mathrm{Kn}_q^j . \tag{2}$$

An effective thermal conductivity and viscosity are defined by $q \equiv -K_{\mathrm{eff}}(\partial T/\partial x)$ and $\tau \equiv \mu_{\mathrm{eff}}(\partial V/\partial x)$, respectively. The MH method indicates that K_{eff} and μ_{eff} are independent of Kn_q [2] but depend on Kn_τ [3-5]:

$$K_{\mathrm{eff}}/K = F_K[\mathrm{Kn}_\tau] = 1 - c_K\mathrm{Kn}_\tau^2 + \mathrm{O}[\mathrm{Kn}_\tau^4], \quad \mu_{\mathrm{eff}}/\mu = F_\mu[\mathrm{Kn}_\tau] = 1 - c_\mu\mathrm{Kn}_\tau^2 + \mathrm{O}[\mathrm{Kn}_\tau^4] . \tag{3}$$

In the limit that $\mathrm{Kn}_\tau \to 0$, the a_k/a_1 and b_k/b_1 for $k \geq 2$ are even polynomials of degree $2(k-1)$ [4-5]:

$$\frac{a_k}{a_1} = (-1)^{k-1}\sum_{j=1}^{k-1} A_{kj}\mathrm{Kn}_q^{2j}, \quad \frac{b_k}{b_1} = (-1)^{k-1}\sum_{j=1}^{k-1} B_{kj}\mathrm{Kn}_q^{2j} . \tag{4}$$

The MH method can be used to evaluate the coefficients in the above expressions [6]. Table 2 contains values of c_K , c_μ , the nonzero A_{kj} , and the nonzero B_{kj} for the IPL-Maxwell, VSS-Maxwell ($\omega = 1$, $\alpha = 2.13986$) [14], and VHS-Maxwell ($\omega = 1$, $\alpha = 1$) [7] interactions, where ω is the viscosity-temperature exponent and α is the angular-scattering exponent. In general, $A_{kj} = 0$ when $j < (k-1)/3$.

DSMC METHOD

The Direct Simulation Monte Carlo (DSMC) method of Bird [7] provides an additional method for determining the normal solution [9-13]. DSMC uses computational molecules that move, reflect from walls, and collide with each other to simulate gas behavior. Here, the variable-soft-sphere (VSS) [14] and the variable-hard-sphere (VHS) [7] interactions are used. These interactions exactly represent the hard-sphere interaction and approximate the Maxwell interaction when suitable values are selected for ω and α (see Table 1).

The domain is shown in Figure 1. Table 3 shows the physical and numerical parameters used in the simulations. The gas has the molecular mass and the reference viscosity of argon [11-13]. With a mean free path of $\lambda = \sqrt{\pi}\mu c_m/2p$, the walls are about 42 mean free paths apart, so the normal solution occupies a large fraction of the domain. The effective thermal conductivity and the effective viscosity are determined in each mesh cell:

$$\frac{K}{K_{\mathrm{eff}}} = -\frac{K}{q}\frac{\partial T}{\partial x}, \quad \frac{\mu}{\mu_{\mathrm{eff}}} = \frac{\mu}{\tau}\frac{\partial V}{\partial x}, \quad \frac{K}{K_{\mathrm{ref}}} = \frac{\mu}{\mu_{\mathrm{ref}}} = \left(\frac{T}{T_{\mathrm{ref}}}\right)^{\omega} . \tag{5}$$

The a_k/a_1 and b_k/b_1 are determined from higher-order velocity moments [11-13]:

$$\frac{a_k}{a_1} = \sum_{i=1}^{k}\left(\frac{(-1)^{i-1}k!(5/2)!}{(k-i)!i!(i+3/2)!}\right)\frac{\left\langle \tilde{c}^{2i}\tilde{c}_x \right\rangle}{\left\langle \tilde{c}^2\tilde{c}_x \right\rangle}, \quad \frac{b_k}{b_1} = \sum_{i=1}^{k}\left(\frac{(-1)^{i-1}(k-1)!(5/2)!}{(k-i)!(i-1)!(i+3/2)!}\right)\frac{\left\langle \tilde{c}^{2(i-1)}\tilde{c}_x\tilde{c}_y \right\rangle}{\left\langle \tilde{c}_x\tilde{c}_y \right\rangle} . \tag{6}$$

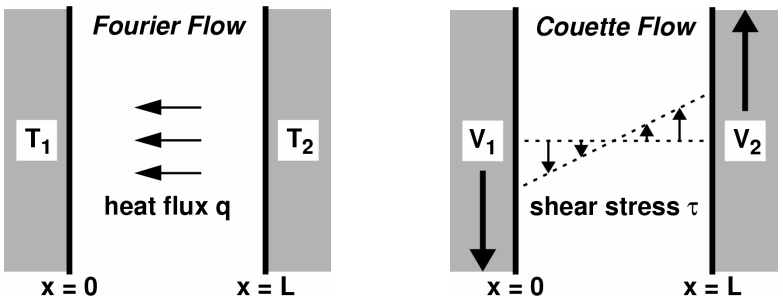

FIGURE 1. Schematic diagrams of Fourier flow (left) and Couette flow (right).

TABLE 1. Chapman-Enskog (CE) results.

Symbol	Hard-Sphere	Maxwell	Symbol	Hard-Sphere	Maxwell	Symbol	Hard-Sphere	Maxwell
ω	1/2	1	a_1/a_1	1	1	b_1/b_1	1	1
α	1	2.13986	a_2/a_1	0.0954284	0	b_2/b_1	0.0617421	0
μ_∞/μ_1	1.016034	1	a_3/a_1	0.0217503	0	b_3/b_1	0.0103303	0
K_∞/K_1	1.025218	1	a_4/a_1	0.0068579	0	b_4/b_1	0.0025919	0
D_∞/D_1	1.018954	1	a_5/a_1	0.0025926	0	b_5/b_1	0.0008207	0

TABLE 2. Moment-hierarchy (MH) results.

Symbol	IPL-Maxwell	VSS-Maxwell	VHS-Maxwell	Symbol	IPL-Maxwell	VSS-Maxwell	VHS-Maxwell
A_{21}	21.1786	21.3155	21.3190	B_{21}	16.3894	16.5355	16.5392
A_{31}	30.8947	32.4522	32.4917	B_{31}	22.4570	24.1045	24.1472
A_{32}	1455.17	1584.61	1588.02	B_{32}	908.683	1007.93	1010.59
A_{41}	11.1479	12.0749	12.0990	B_{41}	6.61697	7.33624	7.35514
A_{42}	4539.44	5272.08	5291.97	B_{42}	2685.43	3210.81	3225.37
A_{43}	222458.	288112.	290023.	B_{43}	115761.	154863.	156027.
A_{52}	5514.96	6805.30	6841.24	c_K	29.0383	29.0418	29.0419
A_{53}	1102750.	1553840.	1567410.	c_μ	596/45	596/45	596/45
A_{54}	62913200.	106469000.	107906000.		≈ 13.2444	≈ 13.2444	≈ 13.2444

TABLE 3. DSMC simulation parameters. Boltzmann constant is $k_B = 1.380658\times10^{-23}$ J/K .

Quantity	Symbol	Value	Quantity	Symbol	Value
Molecular mass	m	66.3×10^{-27} kg	Ref. viscosity	μ_{ref}	2.117×10^{-5} Pa · s
Ref. temperature	T_{ref}	273.15 K	Ref. pressure	p_{ref}	266.644 Pa
Init. temperature	T_{init}	T_{ref}	Init. pressure	p_{init}	p_{ref}
Left wall temp.	T_1	$T_{\text{ref}} - \Delta T/2$	Left wall velocity	V_1	$-\Delta V/2$
Right wall temp.	T_2	$T_{\text{ref}} + \Delta T/2$	Right wall velocity	V_2	$\Delta V/2$
Temperature diff.	ΔT	Up to 400 K	Velocity diff.	ΔV	Up to 800 m/s
Domain length	L	1 mm	Molecules/cell	N	120
Cell size	Δx	0.0025 mm	Time step	Δt	7 ns

RESULTS

Figure 2 shows a_k/a_1 and b_k/b_1 profiles for Maxwell molecules at Kn_q values of 0.006 and 0.017 (i.e., $\Delta T = 70$ K and 200 K, with $\Delta V = 100$ m/s). Actually, Kn_q is not uniform but decreases from left to right because $\mathrm{Kn}_q = q/2pc_m$, q and p are uniform, and c_m increases from left to right. At $\mathrm{Kn}_q \approx 0.006$, the DSMC and CE values are in good agreement in the central region, indicating that the normal solution is obtained in this region. At $\mathrm{Kn}_q \approx 0.017$, the DSMC values differ increasingly from the CE values from right to left (i.e., as Kn_q increases). Within the central region, the variations of the a_k/a_1 and the b_k/b_1 with Kn_q represent the normal solution. Thus, a single DSMC simulation provides the normal solution for the Kn_q values in the central region. The same approach is used to determine the dependence of K_{eff}/K and μ_{eff}/μ on Kn_q. However, these quantities remain so close to unity that their values are averaged over the central region to reduce stochastic errors.

Figure 3 shows the a_k/a_1 and b_k/b_1 values for Maxwell molecules as functions of Kn_q. The four clusters of points correspond to four DSMC simulations with $\Delta V = 100$ m/s and $\Delta T = 70$, 200, 300, and 400 K, and the curves are MH results (Equation (4) and Table 2). In all cases, $\mathrm{Kn}_\tau \le 0.005$, which is small. The DSMC VSS-Maxwell and MH VSS-Maxwell values agree closely except for a_4/a_1 and a_5/a_1 at $\Delta T = 400$ K (the largest value), whereas the DSMC VSS-Maxwell and MH IPL-Maxwell values differ increasingly as k increases. While not shown, the DSMC and MH VHS-Maxwell results are nearly identical to their VSS-Maxwell counterparts. The former slight difference between the DSMC and MH values has two causes. First, discretization errors account for about half of this difference based on additional DSMC simulations in which Δx and Δt are halved while N is doubled. Second, the finite value of Kn_τ also accounts for about half of this difference based on additional simulations at twice the value (i.e., at $\Delta V = 200$ m/s). This figure also shows the a_k/a_1 and b_k/b_1 values for hard-sphere molecules as functions of Kn_q. The dependence on Kn_q is similar: coefficient ratios with even values of k decrease with increasing Kn_q, whereas coefficient ratios with odd values of k increase with increasing Kn_q. However, the rate of change is more gradual for hard-sphere molecules than it is for Maxwell molecules.

Figure 4 shows the K_{eff}/K and μ_{eff}/μ values for Maxwell molecules as functions of Kn_q at several values of Kn_τ. The four symbols along each curve in the thermal-conductivity plots are values from simulations identical to those in the previous figure except with $\Delta V = 0$, 100, and 200 m/s. Since the shear stress must be nonzero to determine μ_{eff}, only values from the latter two simulations are present in the viscosity plots. In distinction to Figure 3, the DSMC values in Figure 4 are averaged over the central region, with error bars corresponding to the 95% confidence intervals. As $\mathrm{Kn}_\tau \to 0$, the DSMC values increase upward toward the MH values. The DSMC values exhibit a slight but consistent increase with increasing Kn_q. However, the net increase over the entire range of Kn_q is comparable to the stochastic and discretization errors for these simulations, which are each about ± 0.002. Thus, to within numerical uncertainty, the Maxwell-molecule transport coefficients are independent of heat flux, in agreement with theory [2-5]. This figure also shows the K_{eff}/K and μ_{eff}/μ values for hard-sphere molecules as functions of Kn_q. No exact theoretical results are available for comparison. As for Maxwell molecules, the hard-sphere values increase upward as $\mathrm{Kn}_\tau \to 0$, and this variation is nearly linear. However, the CE values are not obtained except for small values of Kn_q. Instead, K_{eff}/K and μ_{eff}/μ decrease approximately quadratically with increasing Kn_q. The differences observed at the largest Kn_q are slightly larger than the combined effect of discretization and stochastic errors (about ± 0.002 each) and thus appear to be real.

Figure 5 shows the K_{eff}/K and μ_{eff}/μ values for Maxwell molecules as functions of Kn_τ. The points are from DSMC simulations with $\Delta V = 0$-800 m/s in increments of 100 m/s and $\Delta T = 0$ K, and the curves are MH results (Equation (3) and Table 2). As above, the error bars represent the 95% confidence intervals. In the thermal-conductivity plot, the error bars increase as Kn_τ is decreased. This phenomenon results from the fact that the temperature gradients and the heat flux produced by viscous heating are approximately proportional to Kn_τ^2, whereas the stochastic noise does not depend strongly on Kn_τ. In the viscosity plot, the error bars do not depend strongly on Kn_τ because the shear stress is essentially proportional to the velocity gradient. The offset MH results are in excellent agreement with the DSMC results. The small negative offsets (-0.002 for both transport coefficients) presumably represent the DSMC discretization errors (± 0.002). This figure also shows the K_{eff}/K and μ_{eff}/μ values for hard-sphere molecules as functions of Kn_τ. Since no exact theoretical results are available, curves of the form $c_0 + c_2\mathrm{Kn}_\tau^2$ are fit through the DSMC values. The intercepts of these curves lie between 0.001 and 0.002 and presumably represent the discretization errors (± 0.002). Hard-sphere molecules exhibit a weaker dependence on Kn_τ than Maxwell molecules. Nevertheless, the departures of these quantities from unity at large Kn_τ values are significantly larger than the discretization error, the stochastic error, and their combined effect.

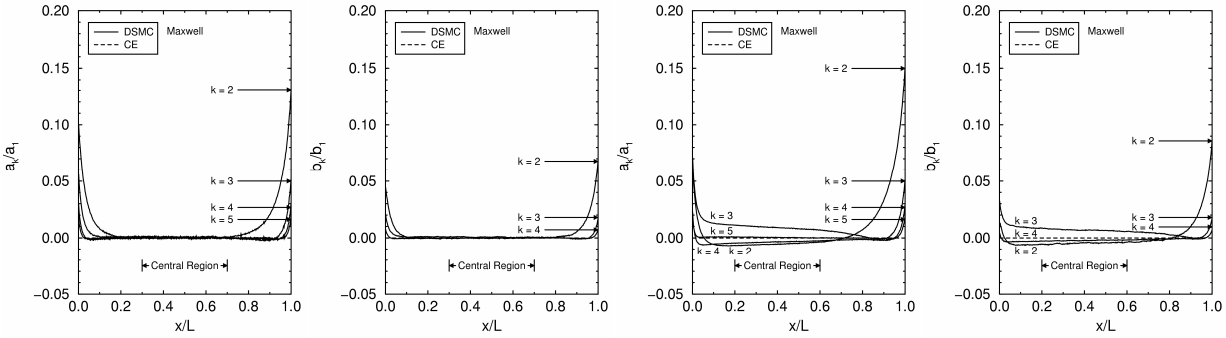

FIGURE 2. Maxwell Sonine-polynomial-coefficient profiles at small (left) and finite (right) Kn_q values.

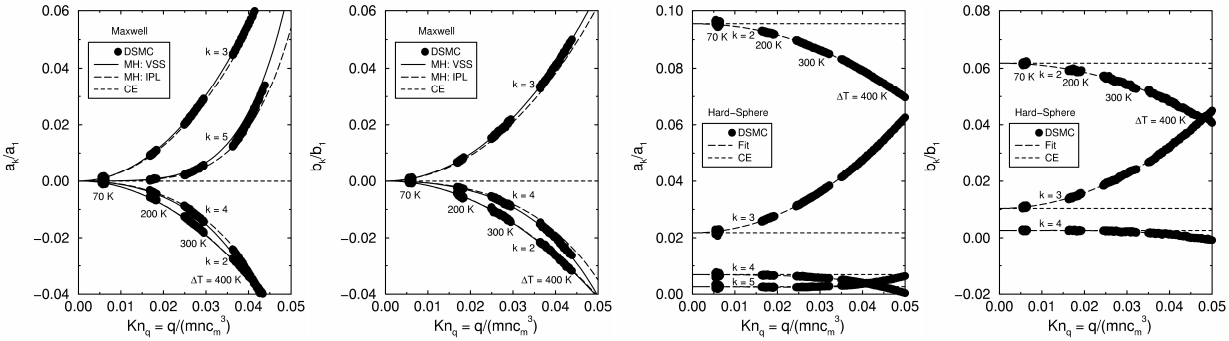

FIGURE 3. Dependence of Maxwell and hard-sphere Sonine-polynomial coefficients on Kn_q.

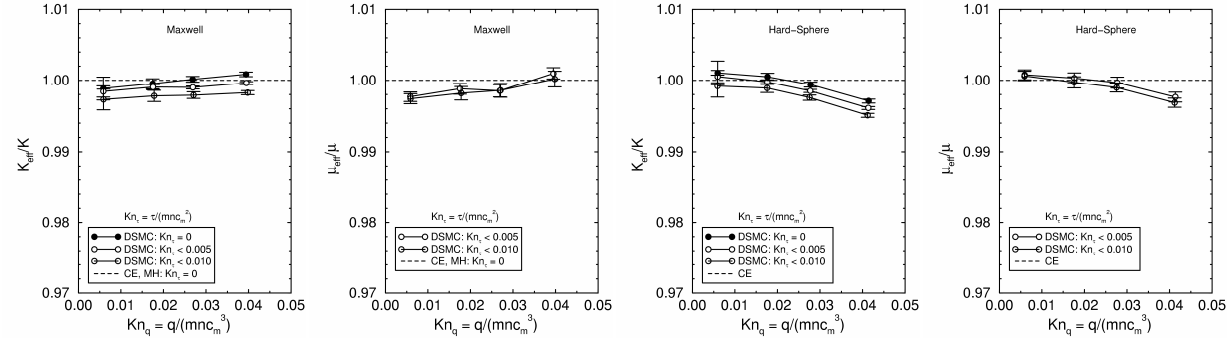

FIGURE 4. Dependence of Maxwell and hard-sphere thermal conductivity and viscosity on Kn_q.

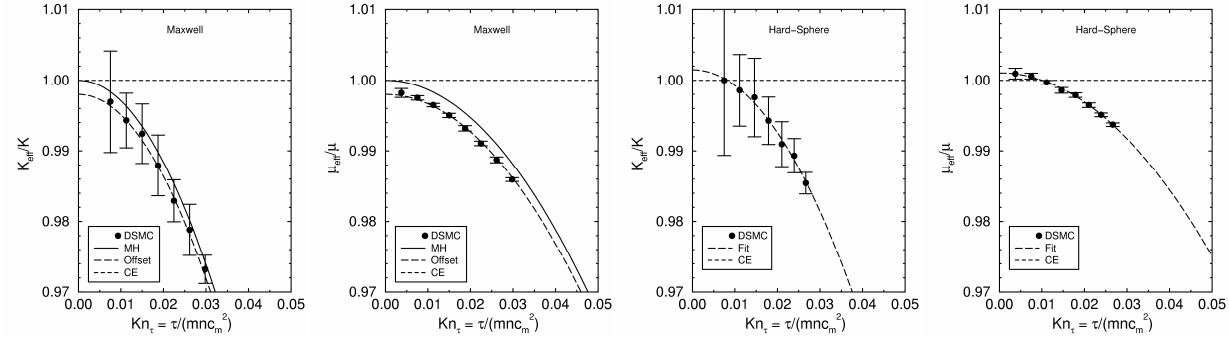

FIGURE 5. Dependence of Maxwell and hard-sphere thermal conductivity and viscosity on Kn_τ.

CONCLUSIONS

The state of a single-species monatomic gas experiencing a large heat flux or a large shear stress is investigated using the moment-hierarchy (MH) method for Maxwell molecules and the Direct Simulation Monte Carlo (DSMC) method of Bird for Maxwell and hard-sphere molecules. Normal solutions of the Boltzmann equation are found for Fourier flow (uniform heat flux) and Couette flow (uniform shear stress) at finite heat-flux and shear-stress Knudsen numbers. The thermal conductivity, the viscosity, and the Sonine-polynomial coefficients from the MH and DSMC methods agree with Chapman-Enskog (CE) theory at small Knudsen numbers. Additionally, these quantities are in agreement at finite Knudsen numbers for VSS-Maxwell and VHS-Maxwell molecules. The MH and DSMC methods both indicate that the effective thermal conductivity and the effective viscosity for Maxwell molecules are independent of the heat-flux Knudsen number but decrease slightly as the shear-stress Knudsen number is increased. Additional DSMC simulations indicate that these transport properties for hard-sphere molecules decrease slightly as the shear-stress Knudsen number or the heat-flux Knudsen number is increased. In all cases examined, these decreases are small, which indicates that the CE values for the thermal conductivity and the viscosity can be used under highly nonequilibrium conditions with small errors so long as the system Knudsen number is small.

ACKNOWLEDGMENTS

Part of this work was performed at Sandia National Laboratories. Sandia is a multiprogram laboratory operated by Sandia Corporation, a Lockheed Martin Company, for the United States Department of Energy's National Nuclear Security Administration under contract DE-AC04-94AL85000. The research of A. S. was supported by the Ministerio de Educación y Ciencia (Spain) through Grant No. FIS2004-01399 (partially financed by FEDER funds).

REFERENCES

1. S. Chapman and T. G. Cowling, *The Mathematical Theory of Non-uniform Gases*, third edition, Cambridge University Press, Cambridge (1970).
2. E. Asmolov, N. K. Makashev, and V. I. Nosik, "Heat Transfer between Parallel Plates in a Gas of Maxwellian Molecules," *Soviet Physics Doklady*, **24**, (11), 892-894 (1979).
3. N. K. Makashev and V. I. Nosik, "Steady Couette Flow (with Heat Transfer) of a Gas of Maxwellian Molecules," *Soviet Physics Doklady*, **25** (8), 589-591 (1981).
4. M. Tij and A. Santos, "Combined Heat and Momentum Transport in a Dilute Gas," *Physics of Fluids*, **7** (11), 2858-2866 (1995).
5. V. Garzó and A. Santos, *Kinetic Theory of Gases in Shear Flows: Nonlinear Transport*, Kluwer Academic Publishers, Dordrecht (2003), Chapters 5 and 6.
6. M. Sabbane and M. Tij, "Calculation Algorithm for the Collisional Moments of the Boltzmann Equation for Maxwell Molecules," *Computer Physics Communications*, **142**, 19-29 (2002).
7. G. A. Bird, *Molecular Gas Dynamics and the Direct Simulation of Gas Flows*, Clarendon Press, Oxford (1994).
8. W. Wagner, "A Convergence Proof for Bird's Direct Simulation Monte Carlo Method for the Boltzmann Equation," *Journal of Statistical Physics*, **66** (3/4), 1011-1044 (1992).
9. J. M. Montanero, M. Alaoui, A. Santos, and V. Garzó, "Monte Carlo Simulation of the Boltzmann Equation for Steady Fourier Flow," *Physical Review E*, **49** (1), 367-375 (1994).
10. J. M. Montanero, A. Santos, and V. Garzó, "Monte Carlo Simulation of Nonlinear Couette Flow in a Dilute Gas," *Physics of Fluids*, **12** (11), 3060-3073 (2000).
11. M. A. Gallis, J. R. Torczynski, and D. J. Rader, "Molecular Gas Dynamics Observations of Chapman-Enskog Behavior and Departures Therefrom in Nonequilibrium Gases," *Physical Review E*, **69**, 042201:1-4 (2004).
12. D. J. Rader, M. A. Gallis, J. R. Torczynski, and W. Wagner, "DSMC Convergence Behavior for Fourier Flow," in *Rarefied Gas Dynamics: 24th International Symposium*, edited by M. Capitelli, American Institute of Physics, Melville (2005), pp. 473-478.
13. M. A. Gallis, J. R. Torczynski, D. J. Rader, M. Tij, and A. Santos, "Normal Solutions of the Boltzmann Equation for Highly Nonequilibrium Fourier Flow and Couette Flow," *Physics of Fluids*, **18**, 017104:1-15 (2006).
14. K. Koura and H. Matsumoto, "Variable Soft Sphere Molecular Model for Air Species," *Physics of Fluids A*, **4** (5), 1083-1085 (1992).